Evaluation of Wireless Resonant Power Transfer Systems With Human Electromagnetic Exposure Limits

Andreas Christ, Mark G. Douglas, *Senior Member, IEEE*, John M. Roman, *Member, IEEE*, Emily B. Cooper, *Member, IEEE*, Alanson P. Sample, *Member, IEEE*, Benjamin H. Waters, *Member, IEEE*, Joshua R. Smith, *Member, IEEE*, and Niels Kuster, *Fellow, IEEE*

***Abstract*—This study provides recommendations for scientifically sound methods of evaluating compliance of wireless power transfer systems with respect to human electromagnetic exposure limits. Methods for both numerical analysis and measurements are discussed. An exposure assessment of a representative wireless power transfer system, under a limited set of operating conditions, is provided in order to estimate the maximum SAR levels. The system operates at low MHz frequencies and it achieves power transfer via near field coupling between two resonant coils located within a few meters of each other. Numerical modeling of the system next to each of four high-resolution anatomical models shows that the local and whole-body SAR limits are generally reached when the transmit coil currents are 0.5 A_{RMS} – 1.2 A_{RMS} at 8 MHz for the maximal-exposure orientation of the coil and 10-mm distance to the body. For the same coil configurations, the exposure can vary by more than 3 dB for different human models. A simplified experimental setup for the exposure evaluation of wireless power transfer systems is also described.**

***Index Terms*—Computer aided analysis, FDTD methods, human exposure, numerical simulation, resonant energy transfer, SAR, wireless power.**

I. Introduction

RECENTLY, efficient wireless high power transfer over relatively long distances between the transmitter and receiver has been achieved with coupled magnetic resonators [1], [2]. Resonant wireless power transfer systems typically operate in the low MHz range (approximately 1–20 MHz). At frequencies below this range, it is difficult to realize high-Q resonant coils with dimensions appropriate for mobile devices, whereas at higher frequencies, the shorter wavelengths limit the spatial extent of the near-field coupling.

The strong reactive near-fields of wireless power systems may induce high fields in the body tissue of persons in their closest vicinity. Therefore, it is important to identify the conditions under which potential product embodiments may demonstrate compliance with international safety guidelines. Insufficient data on exposure to wireless power systems are available in the current literature. Yuan *et al*. [3] evaluated the influence of nearby persons on the transmission efficiency of a wireless power system using simplified models; however, human exposure was not evaluated.

Appropriate metrics for electromagnetic exposure evaluation have not been widely applied in the literature. Some attempted to assess compliance based on incident fields [4], [5]. However, for near-field exposure scenarios, incident field assessment significantly overestimates human exposure [6] and is not suitable for the compliance evaluation of medium and high power systems.

Safety guidelines for EM exposure of workers and of the general public have been issued by the International Commission on Non-Ionizing Radiation Protection (ICNIRP 1998 [7] and 2010 [8]) and the Institute of Electrical and Electronics Engineers (IEEE C95.1-2005 [9]). Above 100 kHz, these guidelines provide basic restrictions for electromagnetic fields in terms of the specific absorption rate (SAR) in the body to prevent whole-body heat stress and excessive localized tissue heating. For the general public, a whole-body averaged SAR limit of 0.08 W/kg and a localized SAR limit of 2 W/kg averaged over 10 g of tissue are provided. The frequency range of interest for wireless power transmission is in a transition region where a second basic restriction is provided to prevent electrostimulation of nerve tissues. SAR limits were applied in this study as they were more relevant for the system investigated.

In this paper, we assess the SAR of a representative wireless power transfer system based on coupled magnetic resonance. Novel numerical and experimental approaches which provide a scientifically sound estimate of the human exposure to such systems are developed.

It should be noted that the potential for tissue heating caused by induced currents in passive or active medical implants are not considered by the current guidelines. A recent study [10]

Manuscript received December 8, 2011; revised May 25, 2012; accepted July 18, 2012. Date of publication October 25, 2012; date of current version April 11, 2013.

A. Christ and M. G. Douglas are with the Foundation for Research on Information Technologies in Society, 8004 Zurich, Switzerland (e-mail: christ@itis.ethz.ch; douglas@itis.ethz.ch).

J. M. Roman and E. B. Cooper are with Intel Corporation, Seattle, WA 98195-2350 USA (e-mail: john.m.roman@intel.com).

A. P. Sample is with University of Washington, Seattle, WA 98195 USA (e-mail: alanson.p.sample@intel.com).

B. H. Waters is with the University of Washington, Seattle, WA 98195 USA (e-mail: bhw2114@uw.edu).

J. R. Smith was with with Intel Corporation, Seattle, WA 98195-2350 USA. He is now with the Department of Computer Science and Engineering and Department of Electrical Engineering, University of Washington, Seattle, WA 98195 USA (e-mail: jrs@cs.washington.edu).

N. Kuster is with the Foundation for Research on Information Technology in Society, 8004 Zurich, Switzerland, and with the Swiss Federal Institute of Technology, 8006 Zurich, Switzerland (e-mail: kuster@itis.ethz.ch).

Color versions of one or more of the figures in this paper are available online at http://ieeexplore.ieee.org.

Digital Object Identifier 10.1109/TEMC.2012.2219870

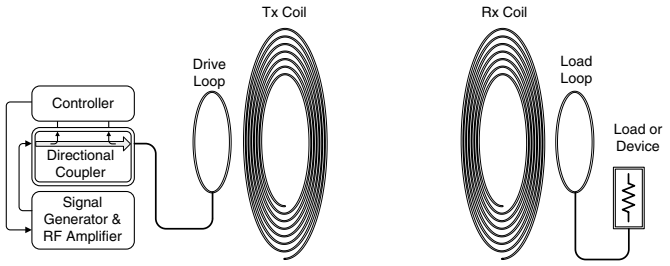

Fig. 1. Schematic block diagram of a magnetically coupled resonant wireless power system. A two element transmitter comprising a loop and high-Q coil wirelessly powers a similar two element receiver. Reprinted from [12], copyright IEEE.

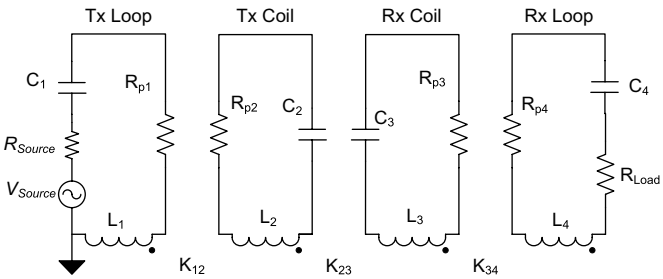

Fig. 2. Equivalent circuit model of the wireless power system. Each of the four antenna elements is modeled as a series resonator. These resonators are linked by their mutual inductances. Reprinted from [12], copyright IEEE.

has shown that localized tissue heating much greater than 1 K may be induced at the tip of an implant lead by RF transmitters in the low MHz frequency range under operating conditions where the basic restrictions for localized induced fields would otherwise be met. The potential for localized tissue heating near implants is a general concern for RF systems, not limited to wireless power. Since the number of factors which can influence potential heating is large, their thorough investigation is beyond the scope of this study.

II. Exposure Assessment

A. Wireless Power System and Lumped Element Model Thereof

In this paper, we consider human exposure to an example wireless power transfer system based on near-field magnetic coupling [11], [12], where power is transferred between two high-quality resonant coils. This model system has dimensions of the same order of magnitude as human length scale and is generally representative of wireless power systems proposed for installation in home, office, or public environments. It is used to illustrate appropriate evaluation methods that are well suited to the independent evaluation of systems of various topologies, geometries, length scales, operating conditions, and exposure configurations.

In the studied configuration, shown schematically in Fig. 1, the drive amplifier is inductively coupled to the transmit coil through a single-turn loop and the load is similarly coupled to the receive coil via an inductive loop, which prevents the source and load from directly loading the resonant coils. The transmit loop has an outer diameter of 305 mm. The transmit coil (TX) is a spiral with 6.1 turns, an outer diameter of 580 mm and a pitch of 10 mm. The loop to coil distance is 135 mm. The diameter of the copper wire is 2.54 mm for the coil and loop. The receive coil and loop (RX) are identical to the transmit coil and loop.

The coupled resonator system can be represented as a lumped-element model shown in Fig. 2 and used to simulate system performance. Lumped circuit component values were extracted from S_{11} data of the TX loop and coil according to the methods described in Sample *et al.* [12] and are summarized in Table I. On the transmit side, the loop is fed with a voltage source with an inner resistance of 50 Ω and a series capacitance of 450 pF for matching. On the receive side, a 50-Ω load resistance is used.

TABLE I
Lumped Element Parameters of the System

R_{p1}, R_{p4}	0.6 Ω
L_1, L_4	1.0 μH
C_1, C_4	450 pF
R_{p2}, R_{p3}	6 Ω
L_2, L_3	39 μH
C_2, C_3	11 pF

Again, a series capacitance of 450 pF matches the loop to the load.

B. Electromagnetic Modeling of the Wireless Power System

For all simulations, the in-house simulation platform SEMCAD X (jointly developed by the IT'IS Foundation and Schmid & Partner Engineering AG, Zürich, Switzerland) is used. The solver is based on the finite-difference time-domain (FDTD) method [13]. The FDTD method is well suited for the simulation of anatomical models because complex tissue distributions can be directly rendered on the computational grid. The local dielectric properties can directly be assigned to the finite difference equation which operates on the respective grid edge. Correctly rendering the wireless power transfer system and the human body models requires mesh step sizes in the order of magnitude of 1–2 mm. Fig. 3 shows the numerical model of the full system as described in Section II-A. Since the coil and the loop are electrically small, the electric losses in the conductors can conveniently be modeled by distributing them to a set of lumped resistances. In the loops, the electric losses in the conductor were not included in the model because they are small with respect to the 50-Ω resistances of the source and the load. SAR averaging is performed according to [14]. All simulations are carried out on highly parallelized graphics processing units which permit the processing of more than 2.5 billion mesh cells per second. For efficiency reasons the Huygens-box approach is used for most dosimetric simulations (see Section II-C).

C. Huygens Box

For the simulation of scattering problems using the FDTD method, the total-field scattered-field (TFSF) method has been proposed [15]. The TFSF method permits one to excite only a limited region of the computational mesh with an incident field which is known *a priori*. The incident field is subtracted on

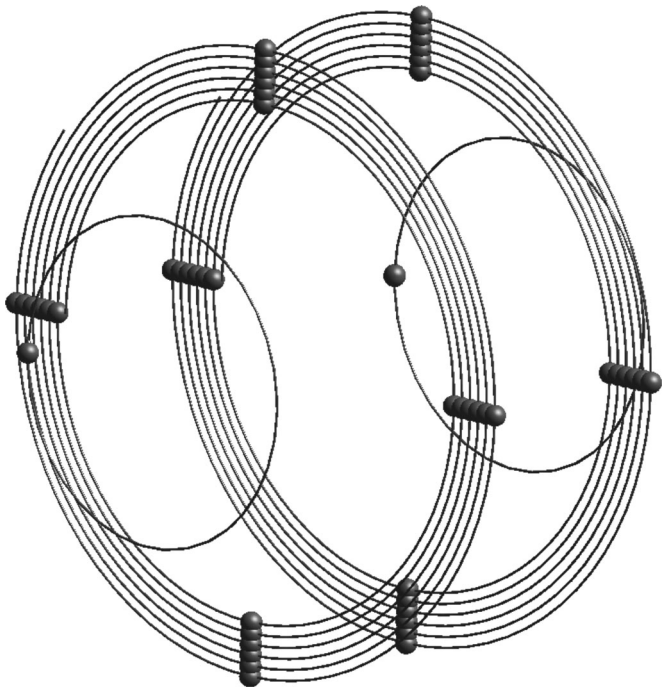

Fig. 3. Numerical model of the wireless power transfer system in the simulation software SEMCAD X. Lumped elements are represented as spheres in the figure.

the boundaries of the TFSF region. Reflections from a scatterer pass through the boundaries of the TFSF region without any distortion, such that the computational domain outside the TFSF region only contains the scattered field. The Huygens box is a generalization of this technique. Complex incident field patterns can be calculated in a single free-space simulation. In a second simulation, the incident field is then applied to the TFSF region (Huygens box) which contains the anatomical body model as the scatterer. This technique is applicable if the impact of the backscattering on the current distributions on the source is negligible or small (see Section III).

D. Anatomical Models

Four detailed anatomical human models were used for the numerical simulations of this study: a male and a female adult, an eight year old girl and a six year old boy, as shown in Fig. 4. Table II summarizes their anatomical characteristics. These models and others were developed within the framework of the Virtual Family Project [16] and several follow up studies. The models are based on high resolution MRI scans (0.5 mm $\times$ 0.5 mm $\times$ 1.0 mm in the head, 0.9 mm $\times$ 0.9 mm $\times$ 2 mm in the trunk and the limbs). They distinguish approximately 80 tissues and organs. The dielectric tissue parameters were taken from the IT'IS tissue database [17] which is largely based on measurements from Gabriel [18].

For the assessment of the exposure with respect to the basic restrictions [7], [9], the four anatomical models were exposed to the single-sided (TX only) wireless power transfer system operating at resonance (8 MHz). For each model, coronal, axial, and sagittal orientations of the coil were analyzed. All models were exposed on their back (see Fig. 5). The nearest distance between the coil and the tissue was 10 mm for all cases.

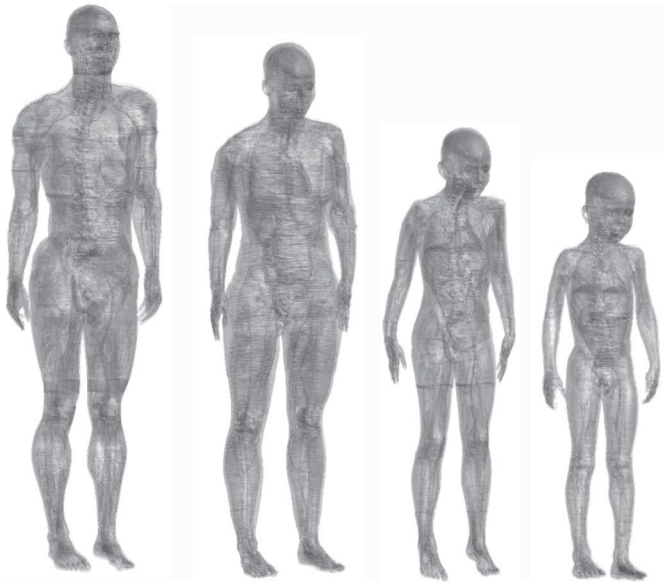

Fig. 4. Anatomical whole body models (from left to right): Duke, Ella, Eartha, Thelonious (see Table II).

TABLE II
CHARACTERISTICS OF THE FOUR ANATOMICAL MODELS

Name	Age (years)	Sex	Height (m)	Weight (kg)	BMI (kg/m^2)
Duke	34	male	1.74	70	23
Ella	26	female	1.60	58	23
Eartha	8	female	1.34	29	16
Thelonious	6	male	1.07	17	15

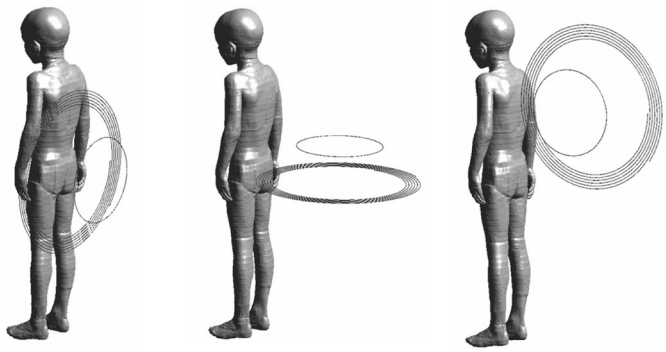

Fig. 5. Orientations of the coil at 10 mm distance to the body (from left to right): coronal, axial, sagittal.

III. VALIDATION

A. Experimental Validation of the Wireless Power System

For the validation of the numerical model of the wireless power system, H- and E-fields were measured for single sided operation (without the receiver side or any other load present) and compared to the numerical results. For the normalization of the results the coil current was measured with a Tektronix AM 503B Current Probe at the mid-point of the coil length.

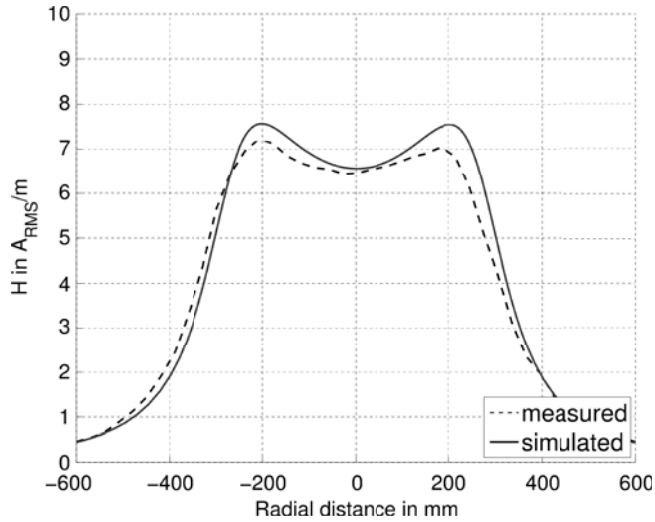

Fig. 6. Measured and simulated magnetic field along a radial line at 100 mm distance in front of the single sided system for a coil current of 1 A_{RMS} at resonance.

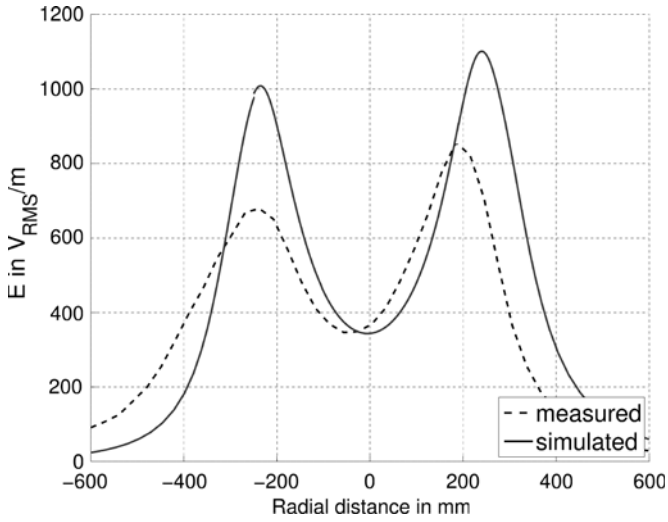

Fig. 7. Measured and simulated electric field along a radial line at 100 mm distance in front of the single sided system for a coil current of 1 A_{RMS} at resonance.

The magnetic fields were measured with a Holaday HI-2200 equipped with a H210 Magnetic Field probe. The isotropy error of this probe is reported by the manufacturer as ± 0.7 dB at 27 MHz, its frequency response is ± 0.8 dB over a frequency range from 300 kHz to 30 MHz. For the measurement of the E-fields, a E100 probe was used with a frequency response of ± 1 dB over a frequency range from 1 MHz to 4 GHz and an isotropy error of ± 0.7 dB at 400 MHz (manufacturer's specification). During measurements, the probes were kept in fixed orientation. The dimensions of the sensor cover of the H-field probe are 60 mm $\times$ 71 mm, the diameter of the cover of the E-field probe is 60 mm. The center points of the sensors are used as reference for the positioning of the probe.

At 100-mm distance, the maximum deviation between measured and simulated H-field at the resonant frequency of 8 MHz is less than 0.7 dB when comparing the respective local maxima (see Fig. 6). This is well within the combined uncertainty. The deviation for the E-field is larger (< 4 dB at the field maxima, Fig. 7). This was expected because a simplified model of the inductive source was used. However, this deviation is not relevant within the context of this paper since the dominant coupling with the human body is due to the magnetic field [6]. Furthermore, the E-field strongly depends on the actual design of the coil.

B. Huygens Box

For the simulations with the Huygens box, the incident field was calculated using a broadband simulation of the unloaded (free-space) single-sided wireless power transfer system. The fields were evaluated using a discrete Fourier transformation (DFT) of the time-domain field components at resonance. These fields were used as incident field for the Huygens Box.

For validation purposes, the spurious scattered field components of an empty Huygens box simulation were evaluated. For this simulation as well as for all following simulations using the anatomical models, a constant mesh resolution of 2.0 mm was used. As mentioned earlier, the fields outside an empty Huygens box should theoretically be zero. Due to numerical uncertainties arising from interpolation and numerical dispersion, certain spurious fields remain in the computational domain. For the configuration and mesh resolution used here, these spurious fields were found to be less than -50 dB of the maximum field amplitude.

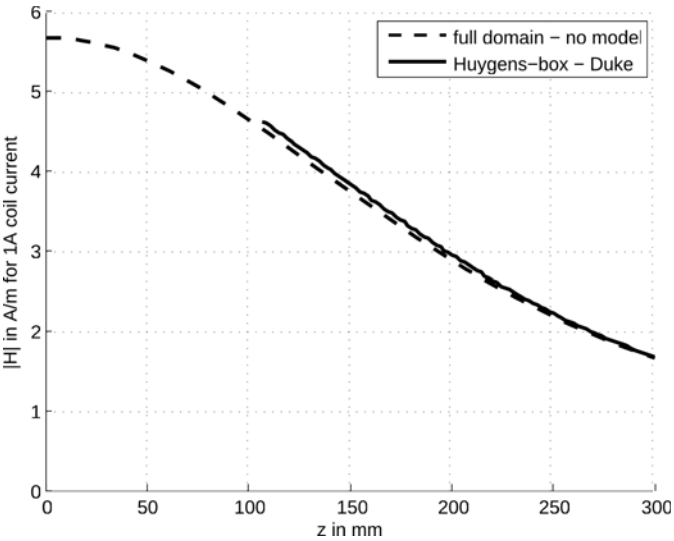

Fig. 8. H-field normalized to 1-A coil current through the center of the unloaded wireless power transfer system (broadband simulation of the entire domain) and of the Huygens-box simulation loaded with the Duke model (harmonic simulation).

The impact of the loading of the transmit coil was evaluated by comparing the H-field distribution of the free space simulation with the H-fields in the Huygens box with the anatomical model of the male adult along the center axis of the system (see Fig. 8). The differences in the H-field distribution are small. Fig. 9 shows the H-field distribution of a full simulation of

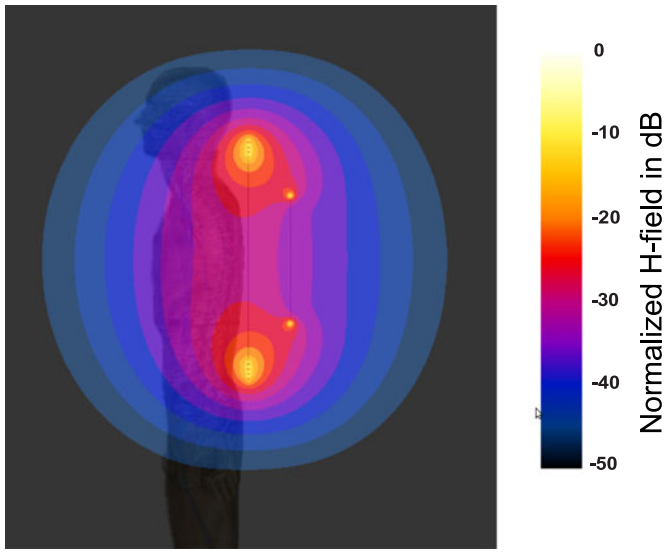

Fig. 9. H-field distribution of a preliminary model of the wireless power transfer system inside and around the anatomical model Duke. It can clearly be seen that the H-field is not distorted by the presence of the body.

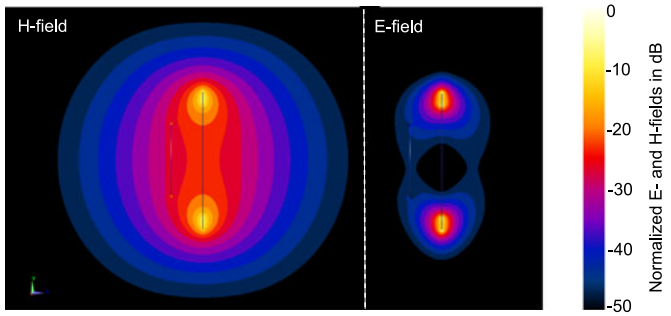

Fig. 10. Distribution of the magnetic and the electric field around a single sided system at resonance.

a preliminary numerical model of the transmit system loaded with the male adult model (no Huygens Box). Although the load represented by the body caused the resonance to decrease by 5%, from 8 to 7.6 MHz, no significant distortion of the H-field can be observed.[1] This confirms the assumptions that the impact of the presence of the model on the current distribution on the coil and—in consequence—on the incident fields is sufficiently small, i.e., the use of the Huygens Box for the dosimetric evaluations is well suited. As the exposure results in this paper are normalized to the coil current, they are not affected by the change in resonant frequency.

IV. Simulation Results

The distribution of the E- and H-fields around the transmit coil at resonance frequency (8.0 MHz) is shown in Fig. 10 without the presence of an anatomical model. The field maxima, which occur near the coil windings, decay faster than exponentially. The decay of H-field is approximately 1–2 dB per 10 mm. The

[1]A similar reduction in resonant frequency in the presence of the body was reported by Yuan *et al.* [3].

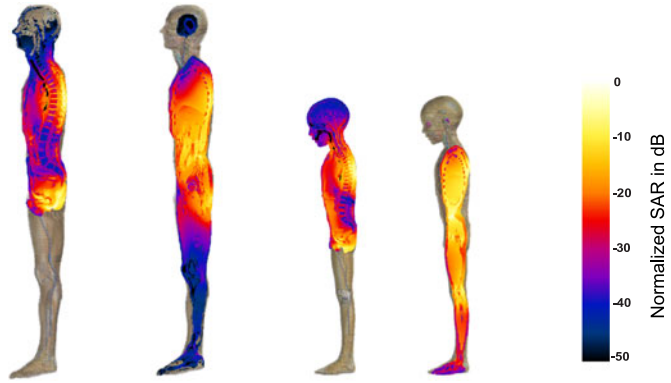

Fig. 11. Local SAR in the models Duke and Thelonious in two sagittal planes (centered and 75 mm off center) for coronal exposure.

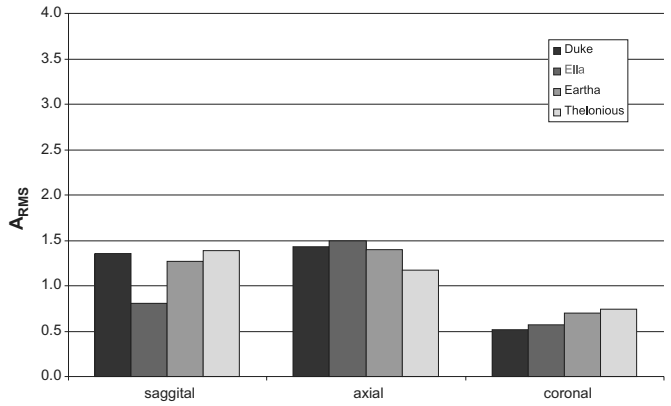

Fig. 12. Current in the transmit coil at which the 1-g SAR limit of 1.6 W/kg is reached [19].

field distributions are asymmetric about the plane of the transmit coil due to the currents on the driving loop.

The peak spatial average SAR and the whole body SAR are evaluated for the configurations described in Section II-D. Fig. 11 shows the distribution of the local SAR in the bodies of the male adult model and the boy model. Whereas the peak spatial average SAR always occurs closest to the coil, the distribution in the body is strongly inhomogeneous and regions of high SAR can occur at larger distances from the coil.

The currents at which the SAR limits for local and whole body exposure are reached for the evaluated configurations are given in Figs. 12–14. Comparing the different loop orientations, the limits are most restrictive for the coronal case because the coil exposes the largest area of the body in this orientation. For the coronal orientation, the exposure limits are generally reached at currents of 0.5 A_{RMS}–1.2 A_{RMS}, depending on the body model and SAR limit used. The 1-g average SAR limit from IEEE C95.1-1999 is the most restrictive limit for the coronal orientation of the coil, followed by the whole-body average SAR limit and then the 10-g average SAR limit of ICNIRP and IEEE C95.1-2005. Variations among different models can exceed 3 dB for the same configurations.

To provide context for the current values at which SAR limits were reached, the transmit coil current was calculated as a function of input power using the model described in Sample

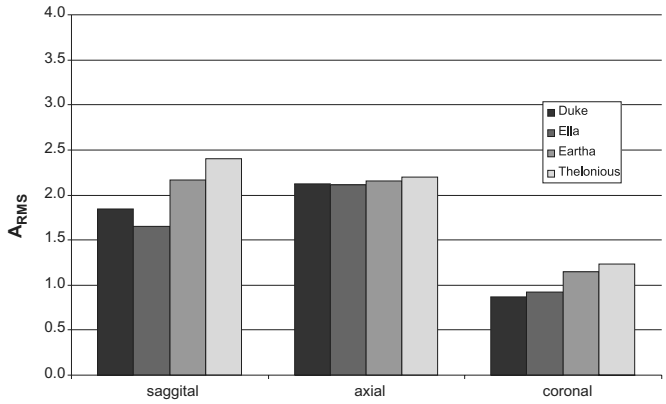

Fig. 13. Current in the transmit coil at which the 10-g SAR limit of 2.0 W/kg in [7] and [9] is reached.

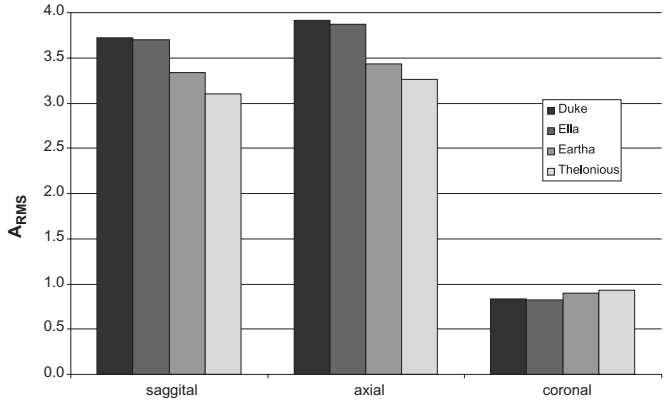

Fig. 14. Current in the transmit coil at which the whole body SAR limit of 0.08 W/kg of [7], [9], and [19] is reached.

et al. [12]. System performance was calculated for the two-sided system (TX and RX) in absence of exposed body. This lumped circuit model only considers the coupling of the adjacent coil or loop elements. Based on the measurement data, we used a loop to coil coupling coefficient of $k_1 = 0.1375$ and a coil to coil coupling coefficient of $k_2 = 0.13$. 0.5 $\mathrm{A_{RMS}}$ corresponds to a transmitted power of approximately 45 W and 1.2 $\mathrm{A_{RMS}}$ corresponds to a transmitted power of approximately 280 W.[2] This provides a preliminary estimate of the transmitted power at which SAR limits are reached for this example system. If the reference levels are applied instead of the basic restrictions, the allowable transmitted power is much lower.

The maximum magnetic field level at 10-mm distance to the transmit coil is approximately 5.7 A/m when the coil current is 1 $\mathrm{A_{RMS}}$ (see Fig. 8). Applying the ICNIRP 1998 reference levels for the general public, the allowable transmit power to meet the reference level for the magnetic field is less than 0.1 W. Applying the reference levels of the Federal Communications Commission (FCC) for the general public [20], the allowable transmit power is less than 0.5 W. Similarly, estimates of the maximum transmit power of a wireless power transfer system developed by Kurs *et al*. [2] have been made in [4]. At a resonant frequency of 10 MHz and a distance of 200 mm from the transmit coil, the incident electric and magnetic fields were measured, and the maximum transmit power was estimated to be more than two orders of magnitude below the power levels calculated in this paper. These results confirm that compliance of wireless power transfer systems with electromagnetic exposure levels can be achieved at significantly higher transmit power than has been estimated based on incident field levels.

[2]The power scales as the square of the current.

V. Dosimetric Measurements

A. Experimental SAR Assessment

The numerical simulation approach described in the previous sections represents a scalable evaluation framework that can be generalized to various transmission devices and receive devices, as well as to various exposure scenarios. Such an approach is particularly useful to evaluate various exposure conditions and to determine where peak exposure is expected.

Dosimetric measurement techniques are commonly used to evaluate SAR compliance to near-field RF sources. Since the actual physical device under test is measured, uncertainties due to device modeling are not an issue. Measurement systems can be designed for low measurement uncertainty, leading to good reproducibility among laboratories. The measurement system can also be designed to provide a conservative estimate of the exposure, so as to cover a known percentile of the user population.

The measurement approach uses a liquid-filled phantom representing the human body. An electric field probe is scanned through the liquid volume and SAR is calculated based on the measured electric field strength. For near-field interaction, the field distribution and the energy absorption in the tissue strongly depend on the orientation of the device and proximity of the user's body. For this reason, application-specific test configurations, positions, and apparatuses are developed to cover exposure scenarios possibly encountered during use.

Such methods have been standardized for compliance measurement of near-field RF sources in the frequency range of 30 MHz–6 GHz such as mobile phones [21], [22] and base stations [23]. In some cases, a mixture of experimental and numerical techniques is applied, such as the exposure assessment of wearers of active implantable medical devices during magnetic resonance imaging [24].

The dielectric properties of the tissue simulating material are designed to represent human tissue while also resulting in a conservative exposure assessment. Different formulations are typically required for different frequency ranges [18]. Tissue simulating liquid recipes are available in the literature above 30 MHz [22]; below 30 MHz, some have used 30 MHz recipes, noting the low rate of change of tissue dielectric properties with frequency at these frequencies [25].

The SAR distribution in a homogeneous phantom will in general be different from that in a human body model, which has many tissues of different dielectric properties. It is therefore important to choose the homogeneous dielectric parameters that provide a conservative estimate of SAR with respect to real

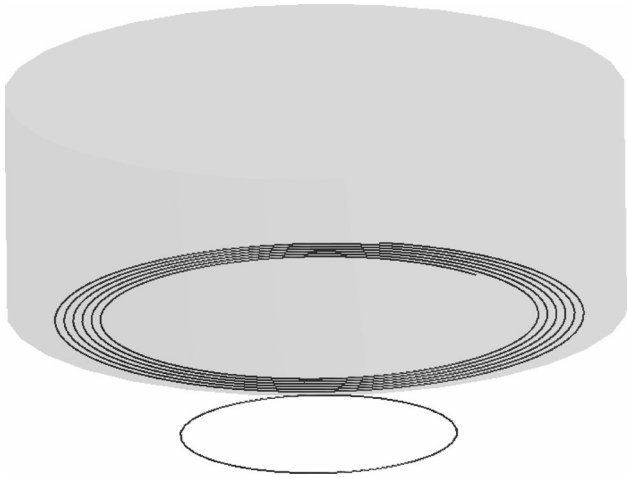

Fig. 15. Cylindrical experimental phantom 10 mm above the coil.

anatomical models. Correction factors may also be introduced to ensure a conservative exposure assessment, as has been proposed in [22] and [23].

B. Phantom Design and Evaluation

To provide a conservative estimate of SAR, the phantom should be designed to correspond to the maximum coupling scenario typically encountered. For example, mobile phones are typically tested at the side of a generic head phantom in order to mimic being held at the head in a talking position or at a flat phantom approximating the exposure for body-mounted use [21], [22]. For the example system described in this paper, we found that the coronal exposure exceeded SAR limits at the most limiting coil currents, so we chose a large cylindrical phantom, which simulates a coronal-type exposure scenario. Such a scenario corresponds, e.g., to a transmitter embedded in a wall and a person standing with his back next to it. Applications with horizontal transmitter deployment, such as mat-type chargers or transmitters embedded in tables are less likely to encounter this exposure scenario. A larger phantom size (e.g., 95th percentile of the body dimensions of the user population) with a flat surface corresponds to a more conservative exposure scenario. Based on population body size data [26]–[30], a diameter of 650 mm and a depth of 250 mm were chosen. The diameter and depth of the phantom are in the range of sitting shoulder height (top of the shoulders to the bottom of the gluteal muscle) and chest depth (chest to shoulder blades), respectively, reported for the 95th percentile of adult German men in the 18–25 year age group [27].

The proposed cylindrical phantom for experimental SAR assessment was simulated with the single-sided coil system at a distance of 10 mm from the coil (using the same setup as for the human body models above), as shown in Fig. 15. Dielectric parameters of $\epsilon_r = 200$ and $\sigma = 0.61$ S/m were chosen for this simulation. These parameters closely match the dielectric parameters of muscle tissue at this frequency. Note that appropriate tissue simulating materials would need to be developed and validated for the frequencies of interest.

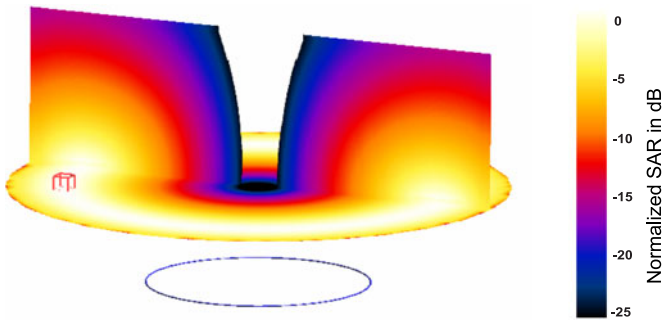

Fig. 16. Distribution of the 10 g spatial average SAR in the phantom.

Due to the presence of the phantom, the resonance frequency of the system shifted from 8.0 MHz to 6.7 MHz, compared to the 0.4 MHz shift observed in the numerical simulation of exposure to a human body model (see Section III-B). Field strength and SAR were evaluated at the modified resonant frequency of 6.7 MHz.

Fig. 16 shows the distribution of the peak spatial average SAR in the phantom. The current in the transmit coil is normalized to the peak 10-g average SAR found in the phantom. For an SAR of 2 W/kg, a current of 0.44 A_{RMS} is obtained. This is on the same order of magnitude as the lowest value of 0.85 A_{RMS} found with the anatomical models for the same coil distance and orientation. The lower coil current with the experimental phantom represents a conservative assessment of the exposure, as required. The E-field vector was found to be mainly oriented in the φ-direction.

The application of such a dosimetric measurement system requires the development and validation of appropriate tissue simulating liquids, of correction factors to correlate measurements made in the homogeneous phantom to expected SAR in a heterogeneous body and of correlation factors between the measurement setup and conservative exposure evaluation covering the entire population.[3] Additionally, specific product embodiments and system geometries may require the development of custom measurement setups.

VI. Conclusion

The exposure of a person in the reactive near-field of a wireless power transfer system has been investigated in this study with the objective to provide recommendations for the scientifically sound evaluation of wireless power transfer systems with respect to human exposure limits. A generic wireless power transfer system was modeled numerically with the transmit coil located 10 mm from each of four anatomical models. For the coronal orientation of the loop, exposure limits are most restrictive. The exposure is strongly dependent on distance and coil design. A dosimetric measurement setup has also been discussed. It was found that the coil current achieving a 10-g average SAR in the phantom at the exposure limit was lower and of the same order of magnitude as the coil current for the anatomical models under similar exposure conditions.

[3]Often the 95th percentile of the population is used as criterium.

There are several key issues that should be addressed before compliance with safety guidelines can be thoroughly demonstrated for any particular product embodiment:

1) evaluation of exposure as function of the coil distance, position relative to the body, and inner anatomy, orientation relative to the body, and body posture in order to ensure that the exposure can be conservatively assessed with the experimental method;
2) evaluation of exposure to the full system including the receiving coil and simulation of system performance accounting for human presence;
3) development of a methodology for exposure assessment (measurement techniques or simulations) that evaluates the exposure with known uncertainty;
4) risk analysis for induced heating near medical implants.

The dosimetric methods described in this paper are generally applicable to wireless power transfer systems of various geometries. For near-field exposure scenarios encountered with these systems, compliance with the safety limits is more accurately evaluated by the direct comparison of the SAR values with the basic restrictions than indirectly in terms of incident field reference levels.

REFERENCES

[1] A. Karalis, J. Joannopoulos, and M. Soljacic, "Efficient wireless nonradiative mid-range energy transfer," *Annal. Phys.*, vol. 323, no. 1, pp. 34–48, 2008.

[2] A. Kurs, A. Karalis, R. Moffatt, J. D. Joannopoulos, P. Fisher, and M. Soljacic, "Wireless power transfer via strongly coupled magnetic resonances," *Science*, vol. 317, no. 5834, pp. 83–86, 2007.

[3] Q. Yuan, Y. Chen, L. Li, and K. Sawaya, "Numerical analysis on transmission efficiency of evanescent resonant coupling wireless power transfer system," *IEEE Trans. Antennas Propag.*, vol. 58, no. 5, pp. 1751–1758, May 2010.

[4] D. Schneider, "A critical look at wireless power," *IEEE Spectr.*, vol. 47, no. 5, pp. 34–39, May 2010.

[5] D. van Wageningen and E. Waffenschmidt. (2009). "Maximum power transfer into space limited by ICNIRP recommendations," [Online]. Available:http://www.wirelesspowerconsortium.com/technology/maximum-power-transfe r-into-space.html

[6] N. Kuster and Q. Balzano, "Energy absorption mechanism by biological bodies in the near field of dipole antennas above 300 MHz," *IEEE Trans. Veh. Technol.*, vol. 41, no. 1, pp. 17–23, Feb. 1992.

[7] ICNIRP, "Guidelines for limiting exposure to time-varying electric, magnetic and electromagnetic fields (up to 300 GHz)," *Health Phys.*, vol. 74, pp. 494–522, 1998

[8] ICNIRP, "Guidelines for limiting exposure to time-varying electric and magnetic fields (1 Hz to 100 kHz)," *Health Phys.*, vol. 99, no. 6, pp. 818–836, 2010

[9] *C95.1-2005 IEEE Standard for Safety Levels with Respect to Human Exposure to Radio Frequency Electromagnetic Fields, 3 kHz to 300 GHz*, IEEE SCC28, IEEE Standards Department, International Committee on Electromagnetic Safety, The Institute of Electrical and Electronics Engineers, New York, NY, 2005

[10] K. Kyriakou, A. Christ, E. Neufeld, and N. Kuster, "Local tissue temperature increase of a generic implant compared to the basic restrictions defined in safety guidelines," *Bioelectromagnetics*, vol. 33, no. 5, pp. 366–374, Jul. 2012.

[11] J. Smith, A. Sample, and E. Cooper, "Flat, asymmetric, and e-field confined wireless power transfer apparatus and method thereof," US-Patent Nr. 2010/0 052 811 A1, Mar. 2010

[12] A. Sample, D. Meyer, and J. Smith, "Analysis, experimental results, and range adaptation of magnetically coupled resonators for wireless power transfer," *IEEE Trans. Ind. Electron.*, vol. 58, no. 2, pp. 544–554, Feb. 2010.

[13] A. Taflove and S. C. Hagness, *Computational Electromagnetics: The Finite-Difference Time-Domain Method*, 2nd ed. Boston, MA/London, U.K.: Artech House, 2000.

[14] *IEEE Std C95.3 Recommended Practice for Measurements and Computations of Radio Frequency Electromagnetic Fields With Respect to Human Exposure to Such Fields, 100 kHz–300 GHz*, IEEE Standards Department, International Committee on Electromagnetic Safety, The Institute of Electrical and Electronics Engineers, New York, NY, Dec. 2002

[15] K. R. Umashankar and A. Taflove, "A novel method to analyze electromagnetic scattering of complex objects," *IEEE Trans. Electromagn. Compat.*, vol. 24, no. 4, pp. 397–405, Nov. 1982.

[16] A. Christ, W. Kainz, E. G. Hahn, K. Honegger, M. Zefferer, E. Neufeld, W. Rascher, R. Janka, W. Bautz, J. Chen, B. Kiefer, P. Schmitt, H.-P. Hollenbach, J. Shen, M. Oberle, D. Szczerba, A. Kam, J. W. Guag, and N. Kuster, "The virtual family development of surface-based anatomical models of two adults and two children for dosimetric simulations," *Phys. Med. Biol.*, vol. 55, no. 2, pp. N23–N28, Jan. 2010.

[17] P. Hasgall, E. Neufeld, M.-C. Gosselin, A. Klingenböck, and N. Kuster, "IT'IS database for thermal and electromagnetic parameters of biological tissues," Version 2.2, Jul. 11th, 2012. Available:http://www.itis.ethz.ch/database.

[18] C. Gabriel, "Compilation of the dielectric poperties of body tissues at RF and microwwave frequencies," Occupational and environmental health directorate, Radiofrequency Radiation Division, Brooks Air Force Base, TX, Tech. Rep. N.AL/OE-TR-1996-0037, Jun. 1996.

[19] *IEEE Std C95.1 IEEE Standard for Safety Levels With Respect to Human Exposure to Radio Frequency Electromagnetic Fields, 3 kHz to 300 GHz*, IEEE SCC28, IEEE Standards Department, International Committee on Electromagnetic Safety, The Institute of Electrical and Electronics Engineers, New York, NY, 1999.

[20] F. C. C. O. of Engineering Technology, *Supplement C (Ed. 01-01) to OET Bulletin 65 (Ed. 97-01), Evaluating Compliance with FCC Guidelines for Human Exposure to Radiofrequency Electromagnetic Fields, Additional Information for Evaluating Compliance of Mobile and Portable Devices with FCC Limits for Human Exposure to Radiofrequency Emissions*. Washington, DC: FCC, Jun. 2001.

[21] *IEEE 1528-2003, IEEE Recommended Practice for Determining the Peak Spatial-Average Specific Absorption Rate (SAR) in the Human Head from Wireless Communications Devices: Measurement Techniques*, IEEE, Piscataway, NJ, 2005.

[22] *IEC Draft 62209-2, Human Exposure to Radio Frequency Fields from Handheld and Body-Mounted Wireless Communication Devices Human models, Instrumentation, and Procedures Part 2: Procedure to Determine the Specific Absorption Rate (SAR) for Mobile Wireless Communication Devices Used in Close Proximity to the Human Body (Frequency Range of 30 MHz to 6 GHz)*, IEC, Geneva, Switzerland: International Electrotechnical Committee, 2009.

[23] *IEC Draft 62232, Determination of RF fFelds in the Vicinity of Mobile Communication Base Stations for the Purpose of Evaluating Human Exposure*, IEC Geneva, Switzerland: International Electrotechnical Committee, 2009.

[24] ISO/TS 10974, Assessment of the safety of magnetic resonance imaging for patients with an active implantable medical device. International Organization for Standardization (ISO), 2012, Draft Technical Specification.

[25] S. Cecil, G. Schmid, K. Lamedschwandner, J. Morak, G. Schreier, A. Oberleitner, and M. Bammer, "Numerical assessment of specific absorption rate in the human body caused by NFC devices," Apr. 2010, pp. 65–70.

[26] D. P. C. Group, "Weight-height relationships and body mass index: Some observations from the diverse populations collaboration," *Amer. J. Phys. Anthropol.*, vol. 128, no. 1, pp. 220–229, Apr. 2005.

[27] J. Jürgens, "Erhebung anthropometrischer Maße zur Aktualisierung der DIN 33 402-Teil 2 (Survey of anthropometric dimensions for the revision of DIN 33 402 - Part 2)," Tech. Rep., Schriftenreihe der Bundesanstalt für Arbeitsschutz und Arbeitsmedizin, (Monograph issued by the Federal Office for Occupational Safety): Bundesanstalt für Arbeitsschutz und Arbeitsmedizin, 2004.

[28] P. Deurenberg, J. A. Weststrate, and J. C. Seidell, "Body mass index as a measure of body fatness: Age- and sex-specific prediction formulas," *Brit. J. Nutrit.*, vol. 65, pp. 105–114, 1991.

[29] P. Deurenberg, M. Yap, and W. van Staveren, "Body mass index and percent body fat: A meta analysis among different ethnic groups," *Int. J. Obesity*, vol. 22, pp. 1164–1171, 1998.

[30] J. Wang, J. Thornton, M. Russell, S. Burastero, S. Heymsfield, and R. Pierson, "Asians have lower body mass index (BMI) but higher percent body fat than do whites: Comparisons of anthropometric measurements," *Amer. J. Clin. Nutrit.*, vol. 60, pp. 23–28, 1994.

Andreas Christ was born in Offenbach, Germany, in 1968. He received the Dipl. Ing. degree in electrical engineering from the Technical University Darmstadt, Darmstadt, Germany, in 1996, and the Ph.D. degree with Niels Kuster's research group at the Swiss Federal Institute of Technology (ETH), Zürich, Switzerland, in 2003.

He currently continuing his research work in the Numerical Dosimetry Group of the Foundation for Research on Information Technologies in Society. He is involved in the assessment of interaction mechanisms of electromagnetic fields and biological tissue. His further research interests include computational electrodynamics with the finite-difference time-domain method, the development of anatomical models for dosimetric simulations and the numerical modeling of medical devices and in the development of numerical and experimental techniques to evaluate the safety of magnetic resonance imaging for patients with medical implants. He has authored and co-authored more than 20 publications in peer-reviewed journals and presented is work than more than 30 international conferences.

Dr. Christ is a member of IEEE-SA where he chairs the Working Group 1 of Technical Committee 34: Wireless Handset SAR Certification, Subcommittee 2: Computational Techniques.

Mark G. Douglas (S'86–M'98–SM'05) received the B.Eng. degree from the University of Victoria, Victoria, BC, Canada, in 1990, the M.Sc. degree from the University of Calgary, Calgary, AB, Canada, in 1993, and the Ph.D. degree from the University of Victoria in 1998, all in electrical engineering.

His research work in electromagnetic dosimetry has resulted in five patents and more than 70 papers for scientific conferences and peer reviewed journals. Since 2009, he has been a Project Leader at the Foundation for Research on Information Technologies in Society in Zurich Switzerland, where his work includes the development of instrumentation and procedures to assess exposure from electromagnetic sources. These sources include mobile phones, wireless power transmitters, induction cooking stoves, electric motors and industrial induction heaters.

Dr. Douglas serves as the Co-chair of IEEE International Committee for Electromagnetic Safety Technical Committee 34 and the Co-chair of ICES Technical Committee 95 Subcommittee 1. From 2002 to 2009, he was an Engineering Manager in the Corporate Electromagnetic Energy Research Laboratory at Motorola in Ft. Lauderdale, FL, where he led advancements in radiofrequency dosimetry research and testing. Before joining Motorola, he was a Senior Technical Leader with the Antenna Development Group at Ericsson in Raleigh, NC, and a member of the Ericsson EMF Research Group in Stockholm, Sweden.

John M. Roman (M'00) received the M.S. degree in electrical engineering from Florida Atlantic University in 1988.

He has been working for more than 25 years on various spectrum, Broadband, and regulatory policy matters. He is currently the Director of Broadband and regulatory Policy, Intel Corporation, Hillsboro, Oregon. Over that time, he has authored several refereed papers on antennas and electromagnetic compatibility, as well as lead dozens of discussions with global policy regulators on their regulatory and broadband policy strategies. He has also chaired several industry technology working groups, including the Wi Fi Alliance RF Health and Science task group, and the CEA R6.3 WG2 on Wireless Power. In his most current role, he is the Director of Broadband and regulatory policy in Intel's Global Public Policy organization, focusing on broadband, universal service, and technology regulatory matters. He works with global policy regulators and stakeholders to share the latest best regulatory and policy methods to help capitalize on all the benefits that Information Communications Technologies and broadband have to offer to national economies and global citizens.

Emily B. Cooper (M'11) received the S.B. degree in 2000, the M.Eng. degree in 2000, and the Ph.D. degree in 2003 all from the Massachusetts Institute of Technology, Cambridge, where her research focused on the development of MEMS biosensors, applications of novel nanofabrication processes, and computational textiles.

Since 2009, she has been with Intel, Seattle, WA, as a Research Scientist to investigate wireless power. Her current work addresses power reduction for natural user interfaces. Before joining Intel, she was a Technical and Strategic Consultant, applying her sensing and materials background to devices and applications in physiological monitoring, portable power, data storage, environmental sensing, and navigation.

Alanson P. Sample (S'03–M'11) received the B.S. degree in 2005 and the M.S. degree in 2008 and the Ph.D. degree in June of 2011 in electrical engineering all from the University of Washington (UW), Seattle.

He is currently a Postdoctoral Research Associate in the Department of Computer Science and Engineering, UW. Throughout his graduate studies, he was with at Intel Labs, Seattle, WA, as both a Full Time Employee and as an Intern. During his time at Intel, he published several articles on the use of magnetically coupled resonators for wireless power delivery, as well as papers on RFID and ambient RF energy harvesting. He was one of the key contributors to the wireless identification and sensing platform, which was open-sourced in 2009 as part of Intels WISP Challenge. His research interests lie broadly in the area of wireless power including: antenna theory and design, energy harvesting from ambient and deliberate sources, novel sensing and computing elements, and the application of these systems.

Benjamin H. Waters (M'10) received the the B.A. degree in 2010 in physics from Occidental College, Los Angeles, CA, and the B.S. degree in 2010 in electrical engineering from Columbia University, New York, NY, and is currently working toward the M.S. degree in electrical engineering with the University of Washington, Seattle.

As an undergraduate, he was in the Columbia Integrated Systems Laboratory (CISL), Columbia University where he completed research on wireless power transfer. He has several internship experiences with Network Appliance, Arup, and most recently with Intel Labs, Seattle, WA, in 2010, where he continued his research in wireless power transfer. His research interests lie mostly in the field of wireless power, including near-field antenna design, adaptive maximum power point tracking systems, and applications for these systems including biomedical, military, and consumer electronics including WREL and FREE-D projects.

Mr. Waters is a member of Tau Beta Pi and Pi Mu Epsilon.

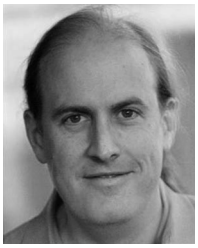

Joshua R. Smith (M'99) received the B.A. degree in computer science and philosophy from Williams College, Williamstown, MA, in 1991, the M.A. degree in physics from Cambridge University, Cambridge, U.K., in 1997, and the S.M. and Ph.D. degrees from the Massachusetts Institute of Technology (M.I.T.) Media Lab, in 1995 and 1999, respectively.

As part of his thesis work at M.I.T., he co-invented an automotive occupant sensor for airbag suppression that that has been standard equipment in all Honda cars since 2000. He is currently an Associate Professor of computer science and electrical engineering, University of Washington (UW), Seattle, where he leads the Sensor Systems Laboratory. His research there focuses on inventing new sensor systems, devising new ways to power them, and developing algorithms for using them. The research has applications in the domains of ubiquitous computing, robotics, medical devices, and Human-Computer Interaction. His group develops novel sensors for robotic manipulation, resonant (nonradiative) wireless power transfer, and (radiative) wirelessly powered sensing platforms. Prior to joining UW, he was a Principal Engineer at Intel Labs, Seattle, WA.

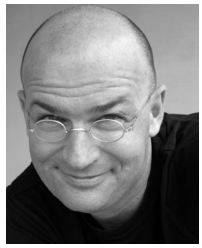

Niels Kuster (F'11) received the M.S. and Ph.D. degrees in electrical engineering from the Swiss Federal Institute of Technology, Zurich (ETHZ), Switzerland, in 1984 and 1992, respectively.

He joined the academic staff of the Department of Electrical Engineering at ETHZ as an Assistant Professor in 1993 and was appointed as a Professor in the Department of Information Technology and Electrical Engineering, ETHZ in 2001. He has been serving as the founding Director of the Foundation for Research on Information Technologies in Society (ITIS), Switzerland, since 2001, and as the President of ITIS USA since its inception in 2010. During his career, he has held invited professorships at the Electromagnetics Laboratory of Motorola, Inc, FL, and at the Metropolitan University, Tokyo, Japan, in 1998. He founded several spin-off companies such as SPEAG, MaxWave, ZurichMedTech, etc. In 2011, he launched a new research initiative, ITIS for Health. His primary research interests include EM technologies, computational life sciences and personalized medicine. His research focuses on the development of: 1) measurement technologies; 2) computational physics; 3) in silico tissue models; 4) physiological human models, 5) medical diagnostic and therapeutic applications, particularly novel cancer treatment modalities; 6) electrodynamics for the optimization of devices operating in highly complex environments, 7) safe and reliable wireless communication links within the body or between implanted devices and external equipment for biometric applications, and 8) exposure setups and quality control procedures for bioexperiments to evaluate interaction mechanisms, therapeutic effects and potential health risks. He has published more than 700 publications (books, journals, and proceedings). He is a member of several standardization bodies and serves as a consultant on the safety of mobile communications for government agencies around the globe.

Dr. Kuster is a Fellow of the IEEE Society, a delegate of the Swiss Academy of Science, and an Associate Editor of IEEE TRANSACTIONS ON ELECTROMAGNETIC COMPATIBILITY. He served as the President of the Bioelectromagnetics Society from 2008 to 2009 and as a member of various editorial boards. In 2012, he received the prestigious d'Arsonval Award, the highest scientific honor of the Bioelectromagnetics Society.